MASTER COPY KEEP FOR REPRODUCTION PURPOSES

REPORT DOCUMENTATION PAGE

Form Approved
OMB No. 0704-0188

1. AGENCY USE ONLY (Leave blank)	2. REPORT DATE	3. REPORT TYPE AND DATES COVERED
		Proceedings 9/29/95-9/28/96

4. TITLE AND SUBTITLE
An International Symposium on Growth and Optical Properties of Semiconductors

5. FUNDING NUMBERS
DAAH04-95-1-0617

6. AUTHOR(S)
Krishan K. Bajaj and T. C. Collins (Organizers)

7. PERFORMING ORGANIZATION NAME(S) AND ADDRESS(ES)
Emory University, Atlanta, GA 30322

8. PERFORMING ORGANIZATION REPORT NUMBER

9. SPONSORING/MONITORING AGENCY NAME(S) AND ADDRESS(ES)
U.S. Army Research Office
P.O. Box 12211
Research Triangle Park, NC 27709-2211

10. SPONSORING/MONITORING AGENCY REPORT NUMBER
ARO 34888.1-EL-CF

11. SUPPLEMENTARY NOTES
The view, opinions and/or findings contained in this report are those of the author(s) and should not be construed as an official Department of the Army position, policy, or decision, unless so designated by other documentation.

12a. DISTRIBUTION/AVAILABILITY STATEMENT
Approved for public release; distribution unlimited

12b. DISTRIBUTION CODE

13. ABSTRACT *(Maximum 200 words)*
The purpose of this symposium was to provide a forum for the discussion of recent developments in the growth and optical studies of III-V and II-VI semiconductors and their heterostructures. Both experimental and theoretical progress in the areas of synthesis, optical characterization and device applications was reviewed by an international panel of distinguished scientists. The future directions of research were discussed. The emergence of enormous interest in the study of wide-bandgap semiconducting systems in recent years and rapid progress made in this area were among the highlights of this symposium. The Symposium was attended by about seventy scientists from U.S., Japan, Germany and France.

14. SUBJECT TERMS
Semiconductors, Optical Properties, Growth, Electronic Devices

15. NUMBER OF PAGES

16. PRICE CODE

17. SECURITY CLASSIFICATION OF REPORT	18. SECURITY CLASSIFICATION OF THIS PAGE	19. SECURITY CLASSIFICATION OF ABSTRACT	20. LIMITATION OF ABSTRACT
UNCLASSIFIED	UNCLASSIFIED	UNCLASSIFIED	UL

DISCLAIMER NOTICE

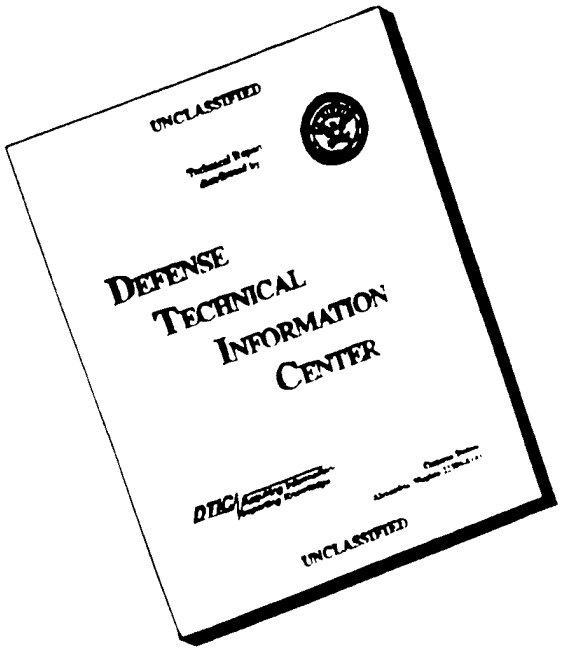

THIS DOCUMENT IS BEST QUALITY AVAILABLE. THE COPY FURNISHED TO DTIC CONTAINED A SIGNIFICANT NUMBER OF PAGES WHICH DO NOT REPRODUCE LEGIBLY.

Proceedings

of

International Symposium

Growth and Optical Properties of Compound Semiconductors

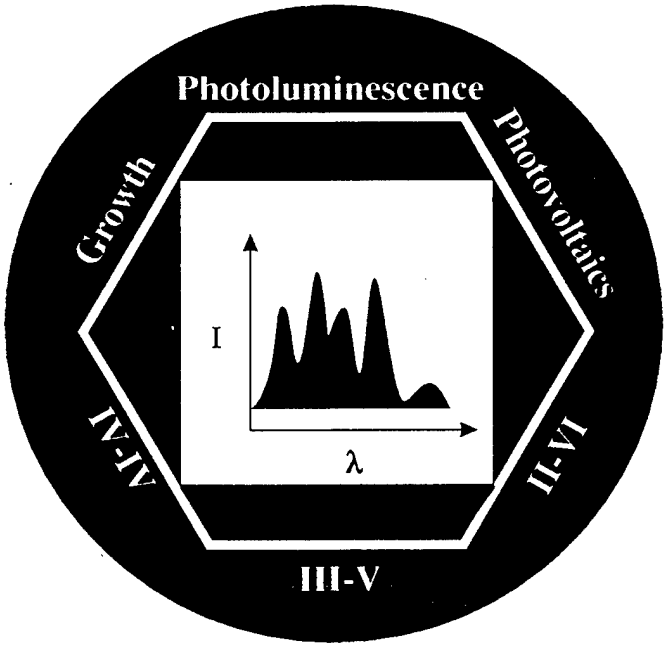

November 13-14
1995
Dayton, Ohio

on the occasion of
Don Reynolds'
75th
Birthday

Organizing Committee

K. K. Bajaj (Emory University, Co-Chair)

T. C. Collins (Oklahoma State University, Co-Chair)

Program Committee

K. K. Bajaj (Emory University)

T. C. Collins (Oklahoma State University)

D. W. Langer (University of Pittsburgh)

C. W. Litton (Wright Patterson Air Force Base)

Y. S. Park (Office of Naval Research)

G. Pomrenke (Advance Research Projects Agency)

J. J. Song (Oklahoma State University)

M. Stroscio (Army Research Office)

G. Witt (Air Force Office of Scientific Research)

Local Arrangements Committee

G. McCoy (Wright Patterson Air Force Base)

D. C. Look (Wright State University)

C. W. Litton (Wright Patterson Air Force Base)

Sponsored by

Air Force Office of Scientific Research (AFOSR)

Office of Naval Research (ONR)

Army Research Office (ARO)

Wright Laboratory (WPAFB, OH)

Emory University

Oklahoma State University

Program

SUNDAY 12 NOVEMBER 1995

EVENING

7:30 - 9:00	**Registration**	
7:30 - 10:00	*Wine & Cheese Reception*	

MONDAY 13 NOVEMBER 1995

MORNING

8:00 - 9:00	**Registration**	
9:00 - 9:15	**Alan Garscadden:**	*Welcome*
9:15 - 9:30	**Jesse Ryles:**	*Welcome*

II - VI BASED OPTO-ELECTRONIC DEVICES: CHAIR - Y. S. PARK

9:30 - 10:00	**K. Böer:**	*The CdS/CuS Solar Cell: From Discovery to Production & Beyond*
10:00 - 10:30	**A. Nurmikko:**	*Prospects for Blue Semiconductor Lasers*
10:30 - 11:00	*Coffee Break*	

Material Issues, Modulation and Ultrafast Spectroscopies: CHAIR - *D. W. Langer*

11:00 - 11:30	**T. Yao**	*Materials Aspects of II-VI Light Emitting Devices*
11:30 - 12:00	**F. Pollak**	*Contactless Electromodulation Spectroscopy of Semiconductor Surfaces and Interfaces*
12:00 - 12:30	**J. Shah**	*Ultrafast Exciton Dynamics in GaAs Quantum Wells*
12:30 - 2:00	*Lunch*	

AFTERNOON

III- V Quantum Confined Structures: CHAIR - *J. J. Song*

2:00 - 2:30	**A. Pinczuk:**	*Light Scattering By Collective Excitations of Quantum Hall Liquids*
2:30 - 3:00	**Y. Chang**	*Optical Properties of Unconfined Excitons in Quantum Wells and Superlattices*
3:00 - 3:30	**J. L. Merz**	*Optical Properties of Self-Assembled Quantum Wires and Quantum Dots*
3:30 - 4:00	*Coffee Break*	

MICROCRYSTALLITES & TRANSITION METAL IONS IN SEMICONDUCTORS: CHAIR - G. POMRENKE

4:00 - 4:30	**T. Goto**	*Optical Properties of Ultrathin PbI_2 Microcrystallites Embedded in Polymers*
4:30 - 5:00	**H. Schulz**	*The Versatile Optical Properties of Vanadium Ions in II-VI and III-V Semiconductors As a Paradigm of 3d Transition Metal Impurities*
5:00 - 6:00	*Poster Viewing*	

EVENING

6:30 - 7:30	**Cocktail Hour**
7:30	*Dinner Banquet*

TUESDAY 14 NOVEMBER 1995

MORNING

BAND STRUCTURE, STRAINED HETEROSTRUCTURES AND CONDENSATION PHENOMENON: CHAIR - D. C. LOOK

9:00 - 9:30	**M. Balkanski**	*Electronic Energy Bands and Lattice Dynamics of Pure and Lithium-Intercalated InSe*
9:30 - 10:00	**M. Dutta:**	*Physics and Devices Applications of Strain Engineered Semiconductor Heterostructures*
10:00 - 10:30	**J. Wolfe:**	*Can The Excitonic Gas in GaAs Display Bose-Einstein Statistics?*
10:30 - 11:00	*Coffee Break*	

SiC AND III - NITRIDES: CHAIR - G. WITT

11:00 - 11:30	**B. Segall:**	*The Conduction Band Edges in 4H and 6H SiC.*
11:30 - 12:00	**H. Morkoc:**	*What is New in GaN Growth and Analysis?*
12:00 - 12:30	**J. Choyke:**	*SiC and III-Nitrides Band Structure, Impurities and Superlattices*
12:30 - 2:00	*Lunch*	

AFTERNOON

GROWTH AND PROPERTIES OF II-VI MATERIALS: CHAIR - C. W. LITTON

2:00 - 2:30	**D. Reynolds:**	*Properties of III-V/II-VI Wide Band Gap Semiconductor Materials*
2:30 - 3:00	**W. Harsch:**	*SPVT™ The Economical II-VI Growth Method*
3:00 - 3:30	**S. Shionoya:**	*Excitonic Molecules in II - VI Compounds: Past, Present and Future*
3:30 - 3:45	*Closing Remarks*	

Curriculum Vitae: Donald C. Reynolds

PROFESSIONAL

Research Scientist	Wright State University, Dayton, Ohio, 1989-
Senior Scientist	Avionics Laboratory, Wright Patterson Air Force Base, Ohio, 1975 - 1989
Director	Solid State Physics Laboratory, Aerospace Research Laboratories, Wright Patterson Air Force Base, Ohio, 1968 - 1975
Supervisory Research Physicist	Aeronautical Research Laboratories, Wright Patterson Air Force Base, Ohio 1952 - 1963
Research Physicist	Battelle Memorial Institute, Columbus, Ohio, 1948 - 1952

EDUCATION

B.S.	Morningside College, Sioux City, Iowa	-1943
M.S.	University of Iowa	-1948

AWARDS

- Air Force Research and Development Command (ARDC) Award for Meritorious Civilian Service, 1958
- Department of Defense (DOD) Distinguished Civilian Service Award, $5,000, 1962
- Harrel V. Noble Award, 1977
- Samuel M. Burka Award, Avionics Laboratory, 1979
- Affiliate Societies Award for Outstanding Professional Achievement, 1982
- Photovoltaic Founders Award, 18th IEEE PVSC 1985

RESEARCH

Experimental Physics:

Condensed Matter. Growth and Characterization of II - VI and III - V Compound Semiconductors, Optical Properties of Compound Semiconductors and Their Heterostructures, Photovoltaics.

Publications:

More than 200 research papers, several review articles and book chapters.
Book: *Excitons: Their Properties and Uses* (with T.C. Collins)
4 Encyclopedia articles
"Direct Solar Energy Conversion by the Photovoltaic Process," statement by D.C. Reynolds presented in the Congressional Record (1974); Requested by Congressman Mike McCormick, Chairman of Subcommittee on Energy

Patents Granted:

"Phospher Composition Containing Indium and Method of Producing Same" 2,676,111
"Phospher Composition Containing Indium and Method of Producing Same" 2,676,112
"Cadmium Sulfide Barrier Layer Cell" 2,844,640
"Apparatus for Growing Single Crystals of CdS and ZnS" 2,907,643
"Method for Growing Single Crystals of CdS and ZnS" 2,947,613
"Photoactive Member for Xerography" 3,121,006
"Photoactive Member for Xerography" 3,121,007
"Cadmium Sulfide Barrier Layer Cell" 2,981,777
"Energy Storage Device" 3,093,735

Abstracts

(Invited Talks)

The CdS/Cu_xS Solar Cell

From Discovery to Production and Beyond

K. W. Böer

Material Science, College of Engineering, University of Delaware, Newark DE 19716

In Honor of Don Reynolds' 75th Birthday

Abstract

With a short *Letter to the Editor* in the *Physical Review*, Don Reynolds reported on September 2, 1954 one of the most important findings for direct solar energy conversion: the "Photovoltaic Effect in Cadmium Sulfide"[1]. At that time the only photovoltaic cells produced were based on selenium and on couprous oxide with a maximum solar conversion efficiency of about 1%, too small to be of commercial interest for large scale terrestrial solar energy utilization. The published data in the CdS-based solar cell indicated a conversion efficiency that is higher by a factor of five, and demonstrates a similar improvement as the single crystal silicon solar cell that was invented in the same year.

However, the CdS/Cu_xS, in contrast to the original Si solar cell can be a polycrystalline, thin-film cell and is relatively easily and inexpensively produced. That makes this cell attractive and stimulated a massive research and development effort worldwide with several thousand publications, dozens of patents[2], and diverse industry groups to attempt mass production.

The first company that produced CdS/Cu_xS solar cells successfully on an industrial scale was the Clevite/Gould Co under Air Force and NASA sponsorship. Don Reynolds was a key player with this research team and significantly helped to create a valid product. The cell efficiency was rapidly improved to exceed 6%, and cells of typically 5"×5" were mass produced. Fred Shirland[3] was in charge of the original development, L.R.Shiozawa *et al.*[4] of the first valid theoretical analysis that prepared the ground for a worldwide drive.

The Institute of Energy Conversion and SES, Inc in Delaware took over the lead in research, achieving in excess of 10% conversion efficiency and installed a semi-automatic production line, working in shifts, with capability of producing 1 MW/year of 8"×8" hermetically sealed cells.

The advantage of these solar cells is the topotaxial exchange reaction that produces on each columnar CdS grain a Djurleite sheat like a jacket crown on a tooth, without interlayers, includes light trapping because of the surface topology, and has, with field-quenching in CdS[5] a build-in field limitation that prevents tunneling-caused junction leakage. A disadvantage is the degradation of the cell that is usually caused by copper nodule formation.

ES, Inc was able to prevent nodule formation at the metal electrode by replacing it with a graphite
]. However, deep crevices that caused needle formation of Cu_xS, originating copper nodules here,
difficult to avoid totally without excessive lowering of the conversion efficiency. This caused a
nercially unacceptable reduction of the production yield of cells with excellent life expectancy (some
ed cells that were produced in 1983 are still alive in outdoor sun exposure with little degradation).
equently SES, Inc shifted its efford to Si solar cells.

he CdS story that started with Don Reynolds, however, does not end here. Today, CdS is used as
player (often referred to as a window) for a variety of commercially attractive solar cells, including
e_2, $CuIn_xGa_{1-x}Se_2$, InP, and CdTe. It is, however, not so much its optical properties (the window-
for this many other materials would qualify; but its ability to show doping saturation in the 100
ange of minority carrier traps that are Coulomb-attractive. It is this feature that permits Frenkel-
excitation well below 100 kV/cm, and thereby space charge elimination to limit fields to below this
hence avoid tunneling-induced junction leaking and thereby permit a much improved solar cell fill
].

REFERENCES

.Reynolds, G.Leies, L.L.Antes, and A.E.Marburger Phys.Rev. **96**, 533 (1954).

.Reynolds, *Encyclopedia of Chemical Technology*, (Interscience Encyclopedia Inc., New York, 1957)
–680 and US Patents No.2848640, July 22 (1958), and No.2981771, April 25 (1961).

hirland, Adv. Energy Conv. **6**, 201 (1966)

.Shiozawa, F.Augustine, G.A.Sullivan, J.M.Smith III, and W.R.Cook, Jr. Final Report, Air Force
t AF33(615), 5224 (1969)

. Böer, *Survey of Semiconductor Physics* (Van Nostrand Reinhold, New York, 1990), Vol I
ns and other Particles in Bulk Semiconductors.

. Böer, U.S.Patent No.4283591, August 11, (1981)

. Böer, *Survey of Semiconductor Physics* (Van Nostrand Reinhold, New York, 1992), Vol II,
Junctions Surfaces and Devices.

Prospects for Blue Semiconductor Lasers

Arto V. Nurmikko and R.L. Gunshor*
Division of Engineering and Department of Physics
Brown University, Providence RI 02912, USA

Compact blue and green semiconductor lasers would impact significantly on such technologies as optical storage and multicolor displays. The availability of a blue semiconductor laser near 450 nm, in conjunction with improvements in encoding topology and superresolution (transcending diffraction limits), is expected to increase the bit density in a compact disk by at least tenfold from that available today. Optical disk storage densities of up to 10 GBit/in^2 are projected over the next decade, comparable to expectations with magnetic disks. Motion pictures, multimedia presentations etc, will be among the direct beneficiaries for a portable medium such as the CD-ROM, linked closely to personal computer technology.

After many early unsuccessful efforts in the 1960s and 70s, the 'natural' material contenders for a short wavelength diode laser, ZnSe and GaN, were deemed hopeless for optoelectronic device applications (and left largely for dead, or for academics, or for dead academics) - until recently. Today, however, one can find laboratory demonstrations of ZnSe-based blue-green cw diode lasers at several research facilities, a deep blue laser has been demonstrated (Fig.1), and a GaN-based blue LED is a commercial reality. Though a number of significant developmental challenges lie ahead, these advances, propelled by new epitaxies and concepts in quantum heterostructures, have profoundly changed the earlier pessimism and expectations of technologists.

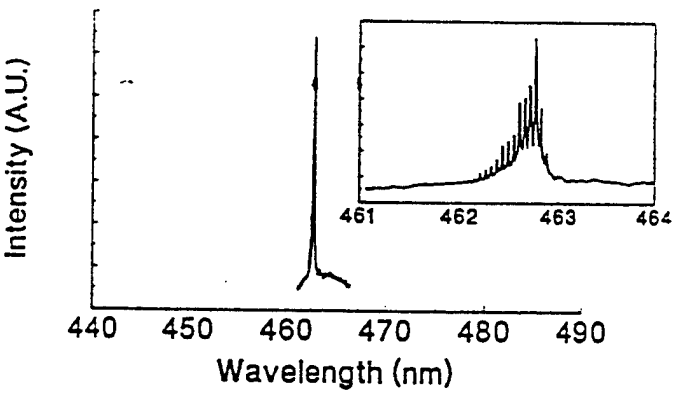

Figure 1: Emission spectrum from a blue II-VI diode laser; inset shows the axial modes (Ref. 1).

A wide bandgap semiconductor would, of course, generally prefer to be a semi-insulator, but can be coaxed into ampotheric electrical activity by insightful synthesis procedures. Yet, in spite of progress e.g in the p-doping of ZnSe and GaN by specific choices of dopants and epitaxies, microscopic understanding of the doping is far from complete. A key question is role of lattice relaxation in the crystal's collective decision making process about a particular acceptor candidate

forming a shallow or a deep level as the bandgap of the material increases (e.g. from ZnSe to ZnMgSSe). A related issue concerns the interplay between point and extended defects in the degradation of present II-VI laser devices, a problem whose solution is of vital importance from a technological point of view.

On the other side of the seesaw, the wide gap semiconductors enjoy fundamentally large interband optical cross sections - an obvious asset for blue light emitters. Excitons and related many electron-hole complexes play an important role in facilitating gain in a ZnSe quantum well, while impurity states coupled strongly to the lattice appear to be of direct benefit to the GaN LED in spite of a highly defected crystal microstructure. In the II-VIs particularly, flexible heterostructure designs have produced, in addition to the advances with the conventional edge emitting lasers, recent demonstrations of vertical cavity surface emitting lasers (Fig.2), and evidence for very large normal mode (vacuum Rabi) splittings in a microcavity in the so-called strong coupling regime. Apart from some fascinating science in photonic nanostructures, these developments add to the design flexibility in the basic optical device infrastructure for wide gap semiconductors.

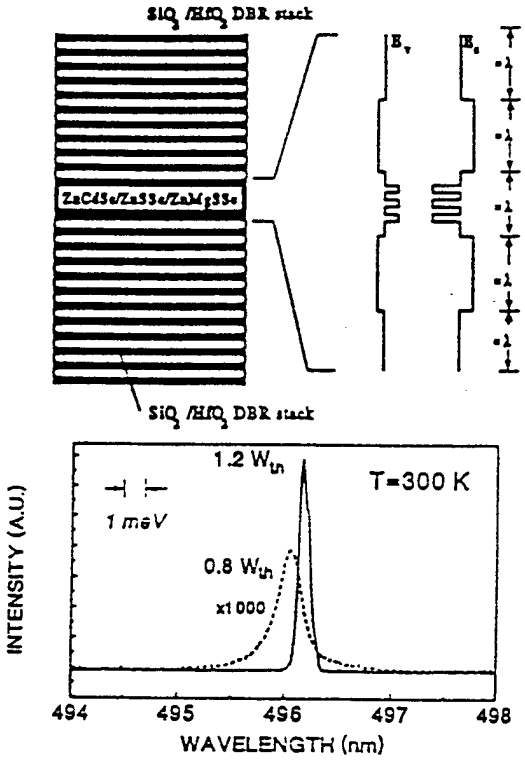

Figure 2: Emission spectra from an optically pumped VCSEL, containing 3 ZnCdSe QWs, below and above threshold of lasing [Ref 2].

Research supported by NSF, ARPA, and AFOSR. We wish to acknowledge Don Reynolds for his impact in launching our journey into the II-VI semiconductors.

*School for Electrical Engineering, Purdue University, West Lafayette IN 47907

[1] D.C. Grillo, J. Han, M. Ringle, G. Hua, R.L. Gunshor, P. Kelkar, V. Kozlov, H. Jeon, and A.V. Nurmikko, Electronics Lett. **25**, 2131 (1994)

[2] H. Jeon, V. Kozlov, P. Kelkar, A.V. Nurmikko, D.Grillo, J. Han, M. Ringle, and R.L. Gunshor, Electronics Lett. **31**, 106 (1995); Appl. Phys. Lett. **67**, 1668 (1995)

Materials aspects of II-VI light emitting devices

Takafumi Yao

Institute for Materials Research, Tohoku University, 2-1-1 Katahira, Aoba-ku, Sendai 980, Japan

Development in materials science and technology triggers new devices which eventually realize novel man-machine systems. We could see such development in the history of II-VI compounds. II-VI compounds have a long
history of electronic materials (fluorescent materials) beginning from the 19th century. Since II-VI compounds have direct bandgaps in the visible region, the materials have basically promising properties for photonic devices. In 1960's, various crystal growth methods were developed mainly for bulk crystals [1], However, serious materials problems arised in terms of electrical properties. As-grown crystals were of high resistivity regardless of doping due to unintentionally incorporated impurities. In order to purify the materials, the Zn extraction method was invented by Aven [2]. We could obtain low-resistive n-type ZnSe and ZnS crystals and p-type ZnTe through Zn extraction but for amphoteric doping. The difficulty in amphoteric doping was explained in terms of the self-compensation mechanism, in which doping-induced vacancies compensate
carriers [3]. The development of epitaxial growth technique enabled one to grow good-crystallinity and high-purity epilayers at low growth temperature, which opened up a new regime of materials science in the end of 1970's [4]. One could grow as-grown low resistivity n-type ZnSe and ZnS as well as p-type ZnTe, but for both types [5]. Most recent development in doping technique has realized amphoteric doping [6], which directly leads to the achievement of a blue-green semiconductor laser diode [7]. Nevertheless, carrier compensation problem still remains challenging to material scientists. Although amphoteric doping became possible, high doping for both conductivity types has not been achieved. For instance, the highest net acceptor concentration (NA - ND) in ZnSe is limited to 1 E18 cm-3 [9], while the highest electron concentration in ZnSe is 2 E20 cm-3 [9]. The carrier compensation problem becomes more serious as the band gap increases [10], which not only prevents the reliable operation of the laser diodes, but also limits the feasibility as photonic device materials. The key issue for the next breakthrough with II-VI's is still conductivity control. In this paper we will address the present status of understanding of the carrier compensation mechanisms.

There have been a number of proposed compensation mechanism mainly from

theoretical side with few from experimental work. The proposed compensation mechanisms are classified into five categories: compensation by native defects [3, 11], complex defects consisting of impurity and proximal native defects [12, 13], impurity associated compensating centers [14 - 17], bond-breaking mechanism [18, 19], and solubility limit [20]. Although there have been a number of proposed compensation mechanisms, it
is obvious that those mechanisms should be examined in the light of experimental results. once we know the compensation mechanism, we, materials scientists, will find a way to overcome the compensation mechanism.

References:

1. "Physics and Chemistry of II-VI Compounds" ed. M. Aven and J.S. Prener (North-Holland, Amsterdam) (1967).
2. M. Aven and H.H. Woodbury, Appl. Phys. Lett. 1, 53 (1962).
3. G. Mandel, Phys. Rev. 134, A1073 (1964).
4. T. Yao et al., Appl. Phys. Lett. 35, 98 (1979).
5. T. Yao, Chap. 10 in "Technology adn Physics of Molecular Beam Epitaxy" ed E.H.C. Parker (Plenum, New York) (1985).
6. K. Ohkawa et al., in Abstracts of 6th Int'l Conf. MBE, San Diego, CA (1990) PIII-21; J. Cryst. Growth 111, 797 (1991). R.M. Parket al., Appl. Phys. Lett. 57, 2127 (1990).
7. M.A. Haase et al., Appl. Phys. Lett. 59, 1272 (1991).
8. J. Qiu et al., Appl. Phys. Lett. 59, 1272 (1991).
9. Z. Zhu, H. Mori, and T. Yao, Appl. Phys. Lett. 61, 2811 (1992).
10. H. Okuyama et al., Appl. Phys. Lett. 64, 904 (1994).
11. D.B. Lax et al., Phys. Rev. B45, 10965 (1992).
12. I.S. Hauksson etal., Appl. Phys. Lett. 61, 2208 (1992).
13. A. Garcia and J.E. Northrup, Phys. Rev. Lett. 74, 1131 (1995).
14. D.J. Chadi, Physica B185, 128 (1993).
15. M. Suzuki, T. Uenoyama, and A. Yamase, Extended Abstracts of 1993 Int'l Conf. Sol. St. Dev. Mat. Chiba (1993) 74.
16. T. Yao et al., J. Cryt. Growth 138, 290 (1994).
17. B.H. Cheong et al., Phys. Rev. B51, 10610 (1995).
18. D. J. Chadi, Appl. Phys. Lett. 59, 3589 (1991).
19. C.H. Park and D.J. Chadi, Phys. Rev. B (August) (1995).
20. D.B. Laks etal., Appl. Phys. Lett. 63, 1375 (1993).

Contactless Electromodulation Spectroscopy of Semiconductor Surfaces and Interfaces

Fred H. Pollak

Physics Department and New York State Center for Advanced Technology in Ultrafast Photonic Materials and Applications

Brooklyn College of CUNY; Brooklyn, NY 11210

Modulation spectroscopy (particularly contactless modes) is a major tool for the study and characterization of semiconductor surface/interfaces [semiconductor/air(vacuum), semiconductor/semiconductor(hetero-and homojunctions), semiconductor/metal, semiconductor/electrolyte] and also for the evaluation of process-induced damage at surfaces/interfaces. For such studies the most useful form of modulation spectroscopy is electromodulation since it is sensitive to surface/interface electric fields and often yields the sharpest structure (third-derivative of the unmodulated spectrum in the case of bulk/thin film material). Furthermore, it can be performed in contactless modes [photoreflectance (PR) and contactless electroreflectance (CER)] that require no special mounting of the sample. Therefore, these techniques can be employed *in-situ* or non-destructively on wafer-sized material. Some recent applications of PR and CER include the investigation of a number of semiconductor surfaces/interfaces such as (a) Fermi level pinning in *n*-and *p*-type GaAs (001) surfaces (including passivation) as well as low temperature GaAs with excess As (buried interfaces), process-induced damage (sputtering, reactive ion etching, chemically assisted ion beam etching), heterojunctions (GaAs/GaAlAs, InGaAs/InP, InAlAs/InP), homojunctions (GaAs/GaAs), semiconductor/electrolyte interfaces and the SiO_2/Si interface in samples prepared by thermal oxidation and subjected to rapid thermal annealing.

This talk will present a recent CER and PR study of *p*-type GaAs (001) structure, fabricated by MBE, which exhibits (a) a reduced surface state density and (b) Fermi level "pinning" values closer to the band edge in relation to other *p*-or *n*-type GaAs (001) surfaces. The effects of the *in-situ* deposition of several monolayers of As on the (001) GaAs surface has been assessed using PR. These results also will be compared with (a) a recent study (in air) of similar MBE fabricated structures, including the effects of etch-induced damage, and (b) the STM work (UHV) of Pashley et al. These investigations also have found reduced surface state densities on *p*-type GaAs (001) in relation to *n*-type material.

From the large number of Franz-Keldysh oscillations observed in CER (from special configurations which contain large, uniform electric fields) the barrier height [$V_B(T)$] has been evaluated over a wide temperature range ($15K < T < 400K$), as shown by the solid squares in the figure. $V_B(T)$ is related to the surface Fermi level [$V_F(T)$] by $V_B(T) = V_F(T) - V_P(T)$, where $V_P(T)$ is the photovoltage. The solid line in the figure is $V_B(T)$, taking into account $V_P(T)$ on the basis of a current transport relationship which contains "pinning" levels at 0.25V and 0.5V above the valence band edge. The fit also yields the surface state density of the two levels. These results will be discussed in terms of the surface chemistry of *p*-type GaAs in relation to *n*-type surfaces.

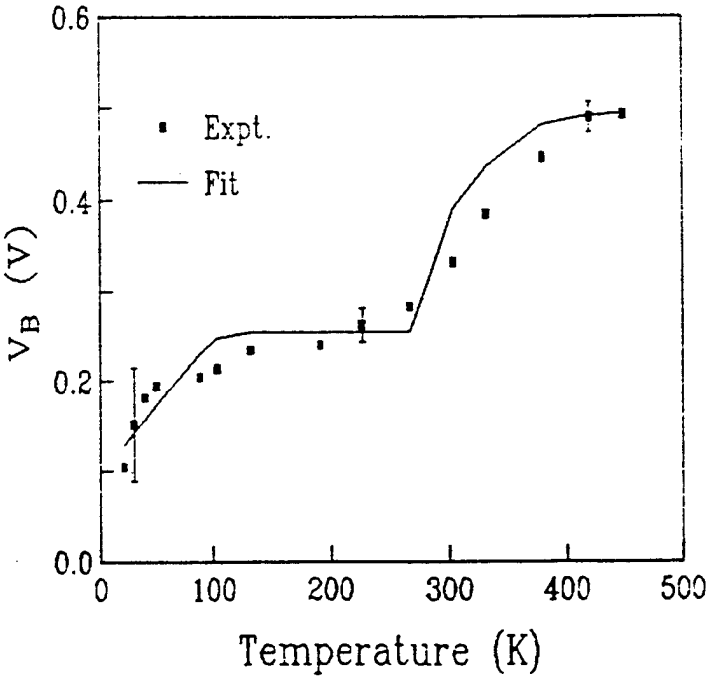

Fig. 1 $V_B(T)$ of a *p*-type GaAs (001) sample. The solid line is a fit to $V_B(T)$, taking into account $V_P(T)$ on the basis of a current transport relationship.

Ultrafast Exciton Dynamics in GaAs Quantum Wells

Jagdeep Shah
AT&T Bell Laboratories
Holmdel, NJ 07733

Excitons have a profound influence on the near-bandgap properties of semiconductors. The enhancement of the exciton binding energy and oscillator strength leads to a more robust exciton in quantum wells. Dynamical properties of excitons in quantum wells have been investigated extensively. However, most of the studies have been performed for non-resonantly excited excitons. In such studies, the dynamics is dominated by the dynamics of exciton formation, thermalization, and cooling. Resonant excitation creates excitons within the homogeneous linewidth of the exciton. These excitons are also non-thermal, but the scattering processes that thermalize them are different. Therefore, resonant and non-resonant excitations probe different aspects of exciton dynamics.

We have recently investigated picosecond [1] and femtosecond [2] dynamics of resonantly-excited excitons. Important results from these studies will be reviewed. Picosecond studies allow us to obtain information about the initial decay dynamics of excitonic emission. The results show that three effects contribute to the results: (1) radiative recombination, (2) spin relaxation, and (3) momentum relaxation. Results for the various polarization components of the emission are compared with a simplified model that contains the essential

physics of the problem. These studies show that a unified model accounting for all these processes is essential for a correct understanding of the relaxation processes. Various scattering rates are determined from these studies.

The femtosecond measurements provide information about the relaxation process occurring immediately after the creation of the exciton. We are able to resolve the rise time of the luminescence and also see femtosecond quantum beats due to heavy and light holes. Interestingly, we find that the exciton momentum scattering time is *shorter* than the exciton dephasing time. The measurements also provide insights into emission versus resonant Rayleigh scattering processes in quantum wells.

[1] A. Vinattieri, J. Shah, T. C. Damen, D. S. Kim, L. N. Pfeiffer, M. Z. Maialle, and L. J. Sham, "Exciton dynamics in GaAs quantum wells under resonant excitation", *Phys. Rev. B* **50**, 10868 (1994).

[2] H. Wang, J. Shah, T. C. Damen, L. N. Pfeiffer, "Spontaneous emission of excitons in GaAs quantum wells: the role of momentum scattering", *Phys. Rev. Lett.* **74**, 3061 (1995).

LIGHT SCATTERING BY COLLECTIVE EXCITATIONS OF QUANTUM HALL LIQUIDS

A. Pinczuk

A.T.&T. Bell Laboratories, Murray Hill, NJ 07974-0636

Research of two-dimensional electron systems in semiconductor quantum structures continues to uncover striking behaviors that arise from the combined effects of strong electron-electron interactions and the reduction in the physical dimensions. The phenomena of the fractional quantum Hall effect, observed in these systems, reveal condensation of the two-dimensional electron gas into novel quantum liquid phases. The fractional quantum Hall effect is an archetype of the intriguing electron quantum fluids that continue to be uncovered in systems of reduced dimensions.

The states of the fractional quantum Hall liquid, as in other quantum liquids encountered in condensed -matter, are expected to support characteristic collective excitations. The electron fluid of the fractional quantum Hall effect is incompressible, in which an energy gap separates the ground state from its excited states. Since at fractional values of Landau level filling factors there are no single-particle gaps, the fractional quantum Hall states are manifestations of the startling effects due to electron interactions. In the incompressible quantum fluid states, the emergence of novel collective gap excitations is the primary consequence of the fundamental new physics involved in these remarkable phenomena[1-3]. The quest for the direct measurement of the collective gap excitations is the major task of spectroscopy in the fractional quantum Hall regime.

Collective gap excitations, or *magnetorotons*[3], of fractional quantum Hall states are observed by resonant inelastic light scattering[4,5]. These experiments offered the first direct evidence of low-energy collective modes predicted by theories of the incompressible quantum fluid. There is another striking element of surprise in the light measurements of q=0 gap excitations. This is because the dynamical structure factor, the function that enters in light scattering cross-sections, vanishes for the small wave vectors in optical experiments.

Since its introduction in 1978[6], the resonant inelastic light scattering method has been used extensively to study free electrons in semiconductor systems of reduced dimensions. The experiments in the fractional quantum Hall regime demonstrate unexpected applications in studies of novel electron quantum fluids. The talk at this International Symposium is an overview of light scattering research that has an impact on the understanding of fundamental electron interactions in quantum Hall liquids. **This presentation is dedicated to Don Reynolds on the occasion of his 75th birthday.**

REFERENCES
(a partial list)

[1] R. B. Laughlin, in *The Quantum Hall Effect*, edited by R. E. Prange and S. M. Girvin, Springer-Verlag, New York 1987, page 233.
[2] F.D.M. Haldane and E.H. Rezayi, Phys. Rev. Lett. *54*,237 (1985).
[3] S.M. Girvin, A.H. MacDonald and P.M. Platzman, Phys. Rev. Lett.*54*,581(1985); Phys. Rev. *B33*,2481(1986).
[4] A. Pinczuk, B.S. Dennis, L.N. Pfeiffer and K.W. West, Phys. Rev. Lett. *70*,3983(1993).
[5] A. Pinczuk, B.S. Dennis, Song He, L.L. Sohn, L.N. Pfeiffer and K.W. West, work in progress.
[6] E. Burstein, A. Pinczuk and S. Buchner, in *Physics of Semiconductors 1978*, edited by B.L.H. Wilson, The Institute of Physics, London 1979, page 1231.

Optical Properties of Unconfined Excitons in Quantum Wells and Superlattices*

Y.-C. Chang, P. Zhao†, and G. Wen‡

University of Illinois at Urbana-Champaign, USA

We report theoretical studies of excitons associated with above-barrier states (unconfined excitons) in semiconductor quantum wells and superlattices. The absorption spectra of these unconfined excitons are calculated and compared with the photoluminescence excitation (PLE) spectra. For the superlattice case, the salient features in the absorption spectra are due to the resonant states localized in the barrier region. By including the subband dispersion and valence-band mixing in a multi-band effective-mass model, the predicted line shapes of the absorption spectra (including fine structures due to mixing of the heavy-hole and light-hole subbands) are found in good agreement with available data.

For the single quantum well case, the above features reduce to the bulk exciton peak associated with the barrier material. However, the center-of-mass (CM) motion of the bulk barrier exciton is modified due to the presence of the quantum well. The interplay of the CM motion and the relative motion is studied in a variational calculation within a one-band effective-mass model, including the effects of the magnetic field. The calculation is done with the use of two sets of trial wave functions. The first set, which describes the CM motion of the unconfined exciton states, includes a spherical 3D exciton wave function multiplied by gaussian-like functions of the CM coordinate in the Z direction. The second set, which describes the confined exciton states, includes a ellipsoidal exciton

wave function (with an anisotropy factor adjusted to model the transition from the 3D to 2D limit) multiplied by the subband envelope functions. To make the computation more efficient, the 3D exciton wave function and the subband envelope functions are all expanded in terms of gaussian-like functions and the Hamiltonian matrix elements between the products of these gaussian functions are calculated analytically.

The coupling of the barrier exciton with the confined exciton via the emission of an optical or acoustical phonon is also examined. The effect of such coupling has been found to play an important role in the photoluminescence and PLE spectra of shallow quantum wells[1]. It was found that the luminescence due to the confined heany-hole exciton is greatly enhanced when the incident photon energy is resonant with the unconfined (barrier) exciton state, indicating a direct coupling of the two states. The dependence of the luminescence intensity on the incident photon energy and on the strength of applied magnetic field is calculated and compared with the experimental observation reported in Ref. [1].

*Work supported by ONR N00014-90-J-1267 and NSF/DMR-89-20538.

† Current address: Dept. of Phys., Stevens Institute of Technology.

‡ Current address: Dept. of Phys., University of Houston.

[1] D.C. Reynolds et al., Phys. Rev. B43, 1871 (1991).

Optical Properties of Self-Assembled Quantum Wires and Quantum Dots

James L. Merz and Peidong Wang
Department of Electrical Engineering
Univ. of Notre Dame, Notre Dame, IN 46556 Phone: 219/631-9177; FAX: 219/631-4393

Pierre M. Petroff
Materials Dept. and Center for Quantized Electronic Structures (QUEST)
Univ. of California, Santa Barbara, CA 93106

Helge Weman
Dept. of Physics and Measurement Technology
Linköping Univ., S-581 83 Linköping, Sweden

Simon Fafard
Institute for Microstructural Sciences
National Research Council of Canada
Ottawa, Ontario, Canada K1A OR6

Because of the difficulties of obtaining arrays of *uniform* nanostructures, such as quantum wires and dots, it would be most desirable to employ some form of self-assembling process to produce these structures. Self-assembly has been pursued at the Center for Quantized Electronic Structures (QUEST). In particular, lateral superlattices have been grown by molecular beam epitaxy (MBE) on vicinal surfaces, and to improve uniformity the growth rate has been varied to produce so-called "serpentine superlattices."[1] In the case of quantum dots, coherently strained InGaAs dots have been grown on GaAs, again by self-assembly.[2]

---

[1] M.S. Miller, H. Weman, C.E. Pryor, M. Krishnamurthy, P.M. Petroff, H. Kroemer, and J.L. Merz, Phys. Rev. Letters **68**, 3464 (8 June 1992).

[2] D. Leonard, M. Krishnamurthy, S. Fafard, J.L. Merz, and P.M. Petroff, J. Vac. Sci. Technol.**B 12**, 1063 (Mar/Apr 1994).

In this talk the optical properties of these wires and dots will be described in detail. For the case of GaAs/AlGaAs serpentine superlattices, extensive polarization measure-ments have been made to demonstrate the one-dimensional nature of these wires, and to determine the extent of intermixing of the Al and Ga components in the wells and barriers. It is found that considerable intermixing takes place, giving rise to weaker exciton binding than was anticipated. The electron of the exciton appears to be 2-dimensional, whereas the hole behaves like a particle in a 1-dimensional structure. Recent magneto-optical measurements[3] have demonstrated that the exciton sees a quantum well in the growth directions, but sees a lateral superlattice in the direction perpendicular to both the wire and growth directions. Furthermore, the exciton binding energy is found to increase from 8 meV for the 2-D case of a quantum well, to 13 meV for a 162 Å quantum wire. Although the confinement of carriers (excitons) in these SSLs is weaker than desired, arrays of these wires are found to be extremely uniform.

In the case of strained InGaAs quantum dots grown on GaAs, relatively strong confinement of carriers is achieved in very uniform arrays of dots.[2] Selective photoluminescence is used to measure subsets of these dots,[4] and further isolation and observation of individual dots has been performed[5] in the AlInAs/AlGaAs material system by etching to remove most of the dots (allowing measurement of only a few hundred, instead of millions of dots), and by cathodoluminescence.[6] Using these methods, luminescence has been observed from single quantum dots, with luminescence linewidths as small as 0.1 meV. Excited state transitions have been observed involving resonant phonon emission, and ground-state saturation effects have been observed.[7] High-field magneto-luminescence measurements will also be reported for these self-assembled dots, as well as the implications of recent capacitance measurements for novel applications will be discussed.

---

[3] H. Weman, E.D. Jones, C.R. McIntyre, M.S. Miller, P.M. Petroff, and J.L. Merz, Superlattices and Microstructures **13**, 5 (1993).

[4] S. Fafard, D. Leonard, J.L. Merz, and P.M. Petroff, Appl. Phys. Letters **65**, 1388 (12 Sept. 1994).

[5] S. Fafard, R. Leon, D. Leonard, J.L. Merz, and P.M. Petroff, Phys. Rev. **B50**, 8086 (15 Sept.1994).

[6] R. Leon, P.M. Petroff, D. Leonard, and S. Fafard, Science **267**, 1966 (31 March 1995).

[7] S. Fafard, private communication

Optical Properties of Ultrathin PbI_2 Microcrystallites Embedded in Polymer

Takenari Goto
Graduate School of Science
Tohoku University
Sendai 980-77, Japan

Exciton and phonon properties characteristic of ultrathin crystal have been studied in PbI_2 microcrystallites. The ultrathin microcrystallites with different thicknesses have been embedded in E-MAA copolymer by Mahler's method [1]. From the TEM photograph, the microcrystallites are found to be platelet like crystals with more than two layers, and to have lateral size of several tens nanometers, where the thickness of the unit layer is 7 Å. Figure 1 shows the absorption spectra at 2K in four polymer films prepared with different heat treatments. Each film contains microcrystallites with different numbers of layers. An average thickness increases in order from sample #1 to #4. The uppermost curve of sample #4 is very similar to the absorption spectrum of the bulk. From the analogy with the bulk spectrum, Bands A, B, C are assigned as due to excitons which are composed of the lowest energy conduction electron with symmetry A_4, the second lowest energy electron $A_{5,6}$, and the third lowest one A_4, respectively. A broad band E is associated with the band-to-band transition. Some peaks appear on the high energy side of the bulk A exciton band at about 2.5eV in the other spectra. These peaks are assigned as due to the exciton formation in the microcrystallites with different layer numbers, and the blue shift originates from size quantization effect on the exciton translational motion in the c-axis direction. Bands B and C shift to the higher energy side with decreasing the average thickness of the microcrystallites. These phenomena are also explained by the size quantization of the exciton energy. The descrete bands, however, are not observed for the sake of the broader band width.

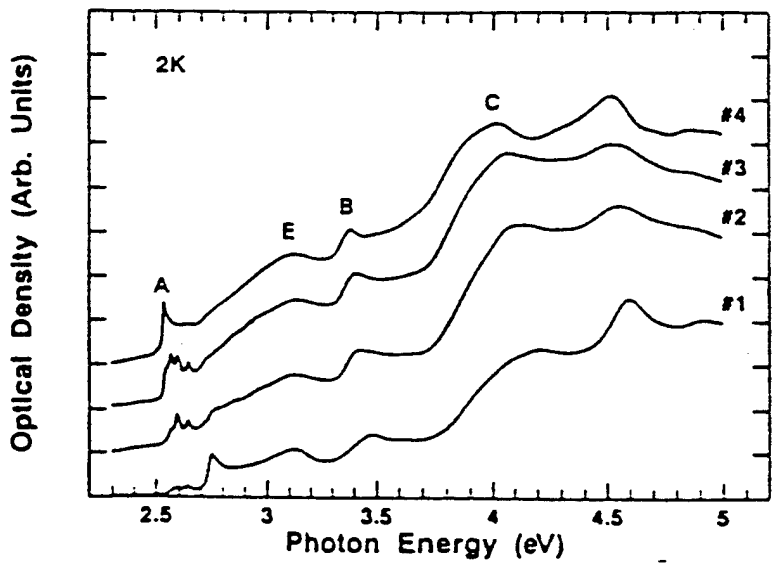

Fig.1 Absorption spectra of the polymer films after different thermal treatments. An average thickness increases from the bottom to the top curve.

In the Raman scattering spectrum where the excitation energy is resonant to the A exciton level, a new line is observed with small Stokes shift less than 21cm^{-1}. Figure 2 shows the Stokes and anti-Stokes resonant Raman spectra of samples #3 and #4 at 77K. In the lowest two curves a and b, the excitation energies locate at the lower energy side of the A-exciton band and at the peak, respectively. The excitation energy of the solid curve between a and i locates within the energy region of the several exciton bands in the absorption spectrum of sample #3 and increases from the lowest solid curve to the highest one. The Raman shift of this line becomes larger when the excitation energy increases. This fact means that the Raman shift becomes larger with decreasing the layer number. In terms of a linear chain model, the phonon energy corresponding to the Raman shift is compared to the calculated phonon energy. It is concluded that this Raman line is associated with a compressional mode of the rigid layer phonon. This phonon is considered to be detected in the resonant Raman scattering because of the strong coupling with the size confined exciton.

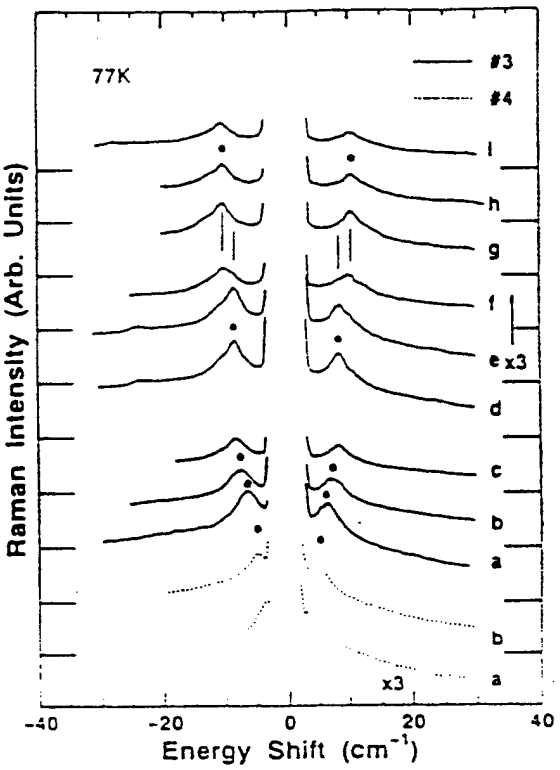

Fig.2 Raman spectra of samples #3 and 4.

In addition, magnetic field dependence of the exciton absorption spectra has been measured in the Faraday configuration at about 10K. From the diamagnetic shifts of the exciton bands in the microcrystallites with 3 and 4 layers, a very large binding energy of the exciton is estimated in the ultrathin crystallites. From this very large binding energy, it is suggested that the wavefunction of the internal motion shrinks in the c-axis direction not only by the size confinement but also by the dielectric screening effect. Since the microcrystallites are surrounded by polymer with the smaller dielectric constant. This shrinkage of the exciton wavefunction is also suggested from the bound exciton luminescence measurements.

References

[1] Y. Wang, A. Suna, W. Mahler and R. Kasowski, J. Chem. Phys. B19, 2305 (1979).

The Versatile Optical Properties of Vanadium Ions in II-VI and III-V Semiconductors as a Paradigm of 3d Transition Metal Impurities

Hans-Joachim Schulz

Fritz-Haber-Institut der Max-Planck-Gesellschaft

Faradayweg 4-6; D-14195 Berlin, FRG

Impurities of the 3d transition elements enter the lattice of compound semiconductors usually in a substitutional position on a cation site. Early studies [1] with II-VI powder materials, demonstrating the utility of vanadium doping for a production of infrared-emitting luminophors, were followed by more thorough investigations of III-V crystals in which the vanadium incorporation was proved by optical and EPR spectroscopies [2]. Presence of vanadium in the quasi-neutral $V^{3+}(d^2)$ state and acceptor-type conversions of the charge state indicated a potential applicability of V-doping for the production of semi-insulating substrate material, although the relevant mid-gap level of GaAs:V was later assigned to a native defect [3,4]. Various experimental and theoretical results evidence Jahn-Teller interaction in the excited V^{3+} states [3,5], while $V^{2+}(d^2)$ exhibits the peculiarity of a low-spin ground state [4].

Starting from an outline of results at III-V compounds, this report will mainly dwell on findings with II-VI materials [6]. ZnS provides the first example of an extensive study emphasizing luminescence identification of both V^{2+} and V^{3+} ions. Not only are the internal transitions detected between the lowest components of the crystal-field-split ground-state

configurations but additionally some light-induced charge-transfer reactions become comprehensible in a one-particle model [7]. ZnSe:V has similar optical properties, however a remarkable deviation in the no-phonon structure of the $V^{2+}(d^3)$ emission [8]. In both these compounds, the ionized acceptor state $V^{-}(d^4)$, too, is detectable by its emission [9]. It is isoelectronic to the more familiar Cr^{2+} ion and also liable to Jahn-Teller interaction. For ZnTe:V the three charge states of the amphoteric V impurity could likewise be established in optical and EPR measurements [10]. Most recent studies of CdTe:V eventually indicate an analogous behavior [11] in spite of earlier speculations arising from the apparent absence of V^{2-} in some samples. Envisaged applications based on the photorefractive effect of this material could entail some technological importance [12].

[1] M. Avinor, G. Meijer: J. Phys. Chem. Solids 12(1960)211

[2] B. Clerjaud: J. Phys. C: Solid State Phys. 18(1985)3615

[3] W. Ulrici, K. Friedland et al.: phys. stat. sol.(b) 131(1985)719

[4] G. Bremond, N. Hizem, G. Guillot et al.: J. Electron. Mater. 18(1989)391

[5] H.-J. Schulz, M. Thiede: J. Phys. C: Solid State Phys. 21(1988)L1033

[6] D.C. Reynolds, C.W. Litton, T.C. Collins: phys. stat. sol. 9(1965)645 & 12(1965)3

[7] S.W. Biernacki, G. Roussos, H.-J. Schulz: J. Phys. C 21(1988)5615

[8] G. Goetz, U.W. Pohl, H.-J. Schulz: J. Phys.: Cond. Matter 4(1992)8253

[9] G. Goetz, U.W. Pohl, H.-J. Schulz et al.: J. Lumin. 60&61(1994)16

[10] P. Peka, M.U. Lehr, H.-J. Schulz et al.: Phys. Rev. B (in print)

[11] P. Peka, H.R. Selber, H.-J. Schulz et al.: to be published

[12] J. Y. Moisan, P. Gravey et al.: Mater. Sci. Engg. B16(1993)257

Electronic Energy Bands and Lattice Dynamics of Pure and Lithium-Intercalated InSe

M. Balkanski,* P. Gomes da Costa† and R. F. Wallis

Department of Physics and Astronomy, University of California, Irvine, CA 92717-4575

Layered semiconductor materials have been investigated for many years.[1] InSe and GaSe have been proposed as possible photovoltaic and photoconductive materials,[2] because their band gaps are relatively large and match the visible spectrum well. More recently, InSe has been considered as a possible cathode material for integrable solid state microbatteries.[3] The remarkable feature for this purpose is the easy intercalation of lithium atoms in the van der Waals gap between layers without significant change in volume. The limiting factor, however, is the electronic conductivity of InSe, especially after intercalation. This property depends on the electronic band structure and lattice dynamics of the material.

The optical absorption spectra of InSe show sharp excitonic peaks at low temperature corresponding to three absorption thresholds. The first threshold at 1.3eV is related to the direct absorption between s, p_z valence band states and s conduction band states. The second at 2.5eV is related to transitions from p_x, p_y valence band states to s conduction band states, and the third at 2.9eV is related to transitions from the spin-orbit split-off valence band to the s conduction band. More recent results on pure InSe at 10K allow one to distinguish the n=1 and n=2 excitonic transitions as well as the LO phonon replica of the n=1 excitonic state.

The excitonic transitions persist after Li insertion, which suggests that all of the Li 2s electrons do not transfer to the conduction band and thus transform the semiconducting InSe into a metal. If we had a metallic transition, the Coulomb interaction between the electron and hole of the exciton would be screened and the excitonic state would be washed

out. The persistence of the excitonic transitions in highly intercalated InSe suggests that the Li 2s electrons form a low mobility impurity band or are efficiently trapped into localized states.

Two aspects of the basic characterization of layered materials with intercalation have been considered: electronic structure and lattice dynamics. Concerning the electronic structure, the tight binding scheme and first principles calculations account well for the magnitude of the direct energy gap in γ-InSe, in spite of the fact that tight binding calculations put it at the center of the Brillouin zone at the Γ point whereas first principles calculations give a direct band gap at the Z point. Generalizations of the tight binding scheme to include the effect of intercalated lithium atoms, with the help of experimental optical absorption data, yield the result that the presence of lithium introduces an impurity band in the energy gap between conduction and valence bands. Furthermore, this band is quite flat, which means that the overlap of the Li electron wave functions with the In and Se atoms is small.

Concerning the lattice dynamics, the model proposed includes short range forces designed to simulate the covalent-band contributions to the potential energy and also long-range Coulomb forces designed to represent those forces whose origin is in the partially ionic nature of the bindings. The model accounts very well for the observed infrared and Raman data for the pure material. The procedure is generalized to lithium intercalated InSe.

---

1. E. Mooser and M. Schlüter, Il Nuovo Cimento B **13**, 164 (1973).

2. A. Segura. Thesis, Université Pierre et Marie Curie, Paris, 1980.

3. M. Balkanski, *Solid State Integrable Microbatteries*, North-Holland, Amsterdam, 1990.

Physics and Device Applications of Strain Engineered Semiconductor Heterostructures

M. Dutta

U. S. Army Research Laboratory, Physical Sciences Directorate
AMSRL-PS-P, Fort Monmouth, New Jersey 07703-5601

Strain in semiconductor devices was initially used to avoid the formation of dislocation and defects in the growth of lattice mismatched materials. The excess energy associated with the strain was thought would encourage dislocation formation and migration. In 1982, Osbourn[1] first proposed that strain in semiconductor was not always bad, it may offer new functionality, whose advantages may far outweigh the disadvantages of the strain. Dramatic improvement in strained-layer devices was predicted[2-4] and many of the predicted advantages have recently been demonstrated.[5-7] Strain-layer structures have been proposed for most major applications: lasers, photodetectors, bipolar transistors and field-effect transistors.

There are usually two kinds of built-in strain associated with in semiconductor devices: latticed mismatch induced and thermal expansion mismatch induced. Thermally induced strain is commonly believed to be bad and hence avoided. Research has concentrated on the lattice mismatch induced biaxial strain. In most cases it is limited to "uniform strain", which does not vary inside the QW along the growth direction. We will discuss the two new kinds of strained structures: 1) an in-plane anisotropic strain, which is thermally induced, 2) a biaxial strain varying along the growth direction, which is lattice mismatch induced, concentrating mainly on the first one. These novel structures exhibit new electronic and optical properties not seen in the conventional strained materials thus they offer new functionalities. In the variable strained quantum well structure,[8] a simultaneous red and blue quantum confined Stark shift of the heavy and light hole transition, respectively has been observed, which may used to control the polarization of the light in the waveguide. In the anisotropic strain quantum well structure,[9,10] an anisotropic absorption with bias tuned polarization rotation and phase retardation has been observed and a high contrast ratio light modulator was demonstrated.[11]

The lattice mismatch induced strain for any (hhk) orientation is biaxial.[12] Anisotropic in-plane strain (e_{xx} ¹ e_{yy}) can only be achieved if a_s ,the lattice constant has a different value for x and y directions, leading to a reduction of the four fold symmetry about a growth axis normal to the (100) oriented substrate, which produces a mixing of the heavy and light hole valence band wave fucntions near k =0. It is achieved in our case by bonding MQW thin film, at temperature T_o, to a new substrate which possesses a direction-dependent thermal expansion coefficient (a_x¹a_y). At a different temperature T¹T_o. a thermally induced strain is induced. Such an in-plan anisotropic strain breaks the rotation symmetry of the valence band at k_x=0, mixing the heavy and light hole bands[10] in the MQW and creating an anisotropic excitonic absorption.[10] This new effect in conjunction with absorption changes produced by the QCSE results in tunable polarization rotation, a new functionality which can be used in a polarization and phase sensitive light modulator.

A 100A GaAs/60A $Al_{0.2}Ga_{0.8}As$ MQW lift-off thin film was bonded to $LiTaO_3$, a transparent substrate with thermal expansion coefficient a_y matching that of the MQW ($6.2x10^{-6}$/°C), while its orthogonal counterpart a_x ($16.2x10^{-6}$/°C) does not. The absorption a_x is significantly different from a_y near the two exciton peaks. The measured birefrigence $Dn=n_x-n_y$ as a function of photon energy is in good agreement with that calculated from the Kramers-Kronig relations using the $Da=a_x-a_y$. For polarization and phase sensitive modulator applications, the MQW was bonded to $LiTaO_3$ at 150°C and operated at room temperature. QCSE is utilized to tune the light polarization rotation and phase retardation created by the in-plane anisotropic strain. The maximum tunable polarization rotation and phase retardation achieved in these experiments were 15° and 37°, respectively. To use the modulator, the incident laser light is linearly polarized at 45° with respect to the strain axis and a polarizer with an orientation perpendicular to the polarization of the transmitted beam in the off state was inserted in the beam path. The emergent light intensity at l=845nm was measured as a function of applied bias, with and without a a polarizer inserted in the beam. With the insertion of the polarizer, the advantage of the polarization rotation and phase retardation were taken into account and the extraordinarily high contrast[11] of 5000:1 was achieved.

One of the most intriguing aspects of these devices is the ultrafast large angle polarization rotation observed on a femtosecond time scale which when compared to the rotation associated with the anisotropic

k-space filling in unstrained GaAs indicates that anisotropic strains as small as 0.2% produce dramatic changes in the polarization dependence of the nonlinear optical properties. Controllable anisotropic strain in conjunction with polarization sensitive nonlinear optical techniques allows for the systematic investigation of the important effects of the reduction of symmetry on the fundamental nature of excitons and exciton-exciton interctions. Femtosecond pump-probe spectoscopy is used to observe a striking polarization dependence of these properties for the resonantly excited lowest heavy-hole-like exciton state of the structure. This dependence is manifested most dramatically at zero time delay for light polarized parallel to the axis of maximum compressive strain through an enhancement of the photoinduced bleaching by greater than one order of magnitude and of the blue shift of the exciton resonance by nearly a factor of two relative to the same quantities measured with orthogonally polarized light. These results imply that the strian-induced anisotropy in k-space leads to exciton-exciton interactions which possess a strong dependence on the orientation with respect to the strain axis, relative orientation and spatial extent of the nonequilibrium excitonic dipoles.

The large anisotropy in the photoinduced bleaching at the measurement energy has been observed which exhibits a strong dependence on the orientation of the probe polarization with respect to the axis of maximum compressive strain (x axis). This result is linked to strain-induced anisotropy in k-space, which for the absorption of linearly polarized light leads to the generation of excitonic dipoles aligned along the electric field vector of the light with spatial extent and therefore scattering rate, phase space filling efficiency and exhange self-energy corrections dictated by the orientation of the light polarization. The polarization dependence is most dramatically illustrated for the experimetnal configuration in which both pump and probe polarizations are parallel to the x axis for which case excitonic dipoles of greatest extent are created. The subpicosecond bleaching decays are attributed to an orientations relaxation of the exicotnic dipoles toward an equilibrium charge distribution determined by the k-space anisotropy.

We have demonstrated that valence band engineering using strain is very powerful, which results in novel and desirable electronic and optical properties not seen in the conventional strained materials. Thus opens new dimensions for optoelectronic device design.

References:

1. G. C. Osbourn, J. Appl. Phys. 53, 1586, (1982)
2. A. R. Adams, Electron Lett. 22, 249, (1986)
3. E. Yablonovitch and E. O. Kane, J. Lightwave Technol. LT-4, 504 (1986)
4. D. Ahn, S. L. Chuang, IEEE J. Q.E. 30, 350 (1994)
5. D. P. Bour, D. B. Gilbert, K. B. Fabian, J. P. Bednarz, and M. Ettenberg. IEEE Photon Technol. Lett. 2 173 (1990)
6. H. K. Choi and C. A. Wang, Appl. Phys. Lett. 57, 321, (1990)
7. R. L. William, M. Dion, F. Chatenoud, and K. Dzurko, Appl. Phys. Lett. 58, 1816 (1991)
8. W. Zhou, H. Shen, J. Pamulapati, P. Cooke, P. Newman, and M. Dutta, CLEO-IQEC'94 (1994).
9. H. Shen, M. Wraback, J. Pamulapati, M. Dutta, P. G. Newman, A. Ballato, and Y. Lu, Appl. Phys. Letts. 62, 2908 (1993)
10. H. Shen, M. Wraback, J. Pamulapati, P. G. Newman, M. Dutta, Y. Lu, and H. C. Kuo, Phys. Rev. B47 (Rapid Comm) 13933 (1993)
11. H. Shen, J. Pamulapati, M. Wraback, M. Dutta, H. C. Kuo and Y. Lu, IEEE Photon Technol.Lett. 6, 700 (1994)

Can the Excitonic Gas in GaAs display Bose-Einstein Statistics?

J.P. Wolfe and J.C. Kim
Physics Department and Materials Research Laboratory
University of Illinois at Urbana-Champaign
Urbana, IL 61801

Abstract

A number of attempts have been made to observe Bose-Einstein Condensation (BEC) of excitonic matter in semiconductors. The rationale for this search is that excitons are thousands of times lighter than atoms and therefore possess thermal De Broglie wavelengths thousands of times longer than those for atoms at the same temperature. When the distance between particles approaches the thermal De Broglie wavelength, the classical Maxwellian distribution of kinetic energies is replaced by a Bose-Einstein distribution.

In most atomic and excitonic systems, attraction between particles causes liquid-gas transitions before the critical density for BEC can be reached. Nevertheless, in 1993, Lin and Wolfe[1] presented evidence for BEC of excitons in Cu_2O, where the band structure precludes the binding of excitons into molecules (and presumably liquid). Just this year, BEC of Rb atoms cooled to nanokelvin temperatures was achieved.[2] Some say that we are on the verge of seeing BEC in a variety of new systems.

Excitons in GaAs, at first thought, would not be particularly promising candidates for observing quantum statistics. First, the excitonic lifetimes are only about half a nanosecond, not much time to thermalize to the crystal temperature. Secondly, the excitonic Bohr radius is rather large -- over 100 Angstroms -- restricting the maximum densities which can be reached before the excitons ionize. Despite these obstacles, we have uncovered an intriguing behavior of the excitonic gas

confined to a quantum well which suggests that at high exciton densities the particles indeed obey Bose-Einstein statistics.

The system under study is a GaAs/AlGaAs multiple quantum well cooled between 2K and 20K and resonantly excited by picosecond laser pulses. At medium to high excitation levels, the time-resolved photoluminescence displays the usual exciton spectrum, accompanied by a lower energy line which we ascribe to the recombination of biexcitons. As the system decays after the laser pulse, the density of the excitonic gas falls and the ratio of excitons to biexcitons closely follows a square-law, implying that chemical and thermal equilibria exist between the two types of particles.[3]

At the highest gas densities, a strange behavior appears: the excitonic signal tends to saturate while the biexciton signal continues to increase, causing a marked deviation from the classical square-law behavior. Theoretical analysis of this two component 2-d gas in the regime of quantum statistics yields a predicted behavior similar to that observed. Basically, as the chemical potential of the gas approaches the zero energy of the biexciton, the exciton population remains relatively constant while the biexciton population is governed by the sharply peaked Bose-Einstein distribution.

Further experiments are required to test this hypothesis. One of the puzzling aspects of this experiment is that the unusual thermodynamic behavior predicted for a nearly ideal gas is observed at densities approaching the close-packing density of excitons.

[1]Lin and Wolfe, Phys. Rev. Lett. 71, 1222 (1993).

[2]Anderson, Ensher, Mattews, Wieman and Cornell, Science 269, 198 (1995).

[3]Kim, Wake and Wolfe, Phys. Rev. B50, 15099 (1994).

The Conduction Band Edges in 4H and 6H SiC

Benjamin Segall and Walter R.L. Lambrecht
Department of Physics, Case Western Reserve University,

For many years there has been a considerable interest in the various polytypes of SiC both from the applied and basic points of view. The interest has heightened recently as material improvements have brought the technological potentialities of SiC closer to realization. It is thus of interest to note that until very recently important information about the nature of the conduction band edge, namely, the location of the conduction band minima and the associated effective masses, in the most abundant and perhaps technologically most important polytypes, 4H and 6H, was quite limited and, in some cases, even controversial. Perhaps the least controversial item was the location of the minimum in 6H. Most experimental evidence suggested a position on the boundary of the hexagonal BZ somewhere on the ML axis. This is in accord with band calculations of the authors[1] who employed the full potential linear muffin-tin orbital (LMTO) method. More specifically, we found the minimum to lie nearly half-way between the symmetry points M and L. This means that there are two minima on each of the three equivalent ML axes. It turns out that the barrier between the two minima is quite low (~10 meV) making the bands in the ML direction rather nonparabolic and the mass rather dependent on energy, or, band filling. In 4H SiC, the situation was more murky for quite a while. Arguments based on the analysis of the phonon replica lines in the photoluminescent decay of excitons bound to N donors[2] lead to the conclusion that the conduction band minimum could not be on the BZ boundary. Our band structure and that of some others, however, indicated that minimum is at the point M. Using phonon spectra for 4H calculated by Hofmann et al[3], it will be shown that the reported phonon replica photoluminescence spectrum in 4H is, in fact, completely consistent with the minimum being at the point M.

One of the earliest reported determinations of the masses in 4H and 6H[4,5] came from an effective mass approximation fit of the excited state IR spectra of the N donors in these materials. The mass tensor was assumed to have axial symmetry. More recently Son et al.[6,7] used the optically detected cyclotron resonance (ODCR) technique on high quality epitaxial film to obtain information about the masses. From the very weak variation of the cyclotron resonance (CR) signal with the direction of B in the basal plane, they concluded that the mass tensor was axially symmetric. This conclusion was in agreement with the assumptions of Refs. 4 and 5. However, the transverse and longitudinal masses they reported differ markedly from those obtained from the donor IR spectra. From fine-grained calculations of the bands in the vicinity of the minima, we determined the mass tensors for both polytypes. It was found that both tensors were totally anisotropic, a fact that is

consistent with the C_{2v} symmetry of the minima. To pursue the comparison with the ODCR results further, we simulated the X-band (9.2 GHz) cyclotron resonance signal (including the experimentally reported broadenings $\omega\tau$) from the several calculated ellipsoidal energy surfaces involved. This required calculating the B field orientation-dependent cyclotron masses for the ellipsoids. For B in the basal plane, we find that the overlapping broadened CR signals from the different ellipsoids merge into a single broad peak which is rather insensitive to the direction of B in the plane. This finding explains Son et al.'s inability to resolve the mass anisotropy in the basal plane. The calculated "effective" transverse and longitudinal masses, $m^*_{\perp} = 0.40$ and $m^*_{||} = 0.27$ for 4H and $m^*_{\perp} = 0.43$ and $m^*_{||} = 1.1\text{-}2.0$ for 6H are in satisfactory accord with the ODCR results. The spread in the longitudinal value for 6H is the energy dependence noted above. We note that our simulations at higher frequencies in the Q band (35GHz) reveal structure corresponding to the in-plane anisotropies. Recently these predictions were confirmed[8] in 4H. Details about the principal and CR masses will be discussed. Finally, we note that recent Hall measurements[9] have indicated a fairly high anistropy in the electron mobility ratio $\mu_{\perp}/\mu_{||}$ of about 3 to 6 for 6H is due to but a much smaller value of roughly 0.7 to 1.0 in 4H SiC. While the mobility ratio is expected to inversely related to the corresponding mass anisotropy, the detailed mass dependence is not simple as the mass dependencies are different in the several scattering mechanisms that are involved in the transport over the temperature range studied. Within that uncertainty, the mobility ratios are reasonably consistent with the calculated mass anisotropy ratios.

1. W.R.L. Lambrecht and B. Segall, Phys. Rev. B52, R2249 (1995).
2. L. Patrick, W. J. Choyke, and D.R. Hamilton, Phys. Rev. 137, A1515 (1965).
3. M. Hofmann, A. Zywietz, K. Karch and F. Bechstedt, Phys. Rev. B50,13401 (1994).
4. W. Suttrop, G. Pensl, W. J. Choyke, R. Stein, and S. Leibenzeder, J. Appl. Phys. 73, 3708 (1992).
5. W. Gotz, A. Schoner, G. Pensl, W. Suttrop, W. J. Choyke, R. Stein and S. Leibenzeder, J. Appl. Phys. 73, 3332 (1993)
6. N. T. Son, W. M. Chen, O. Kordina, A. O. Konstantinov, B. Monemar, E. Janzen, D. M. Hoffmann, D. Volm, M. Drechsler, and B. K. Meyer, Appl. Phys. Lett. 65, 3209 (1994).
7. N. T. Son, O. Kordina, A.O. Konstantinov, W. M. Chen, E. Sorman, B. Monemar, and E. Janzen, Appl. Phys. Lett. 65, 3209 (1994)..
8. B. K. Meyer, private communication.
9. M. Schadt, G. Pensl, R. P. Devaty, W. J. Choyke, R. Stein, and D. Stephani, Appl. Phys. Lett. 65, 3120 (1994).

What is new in GaN Growth and Analysis?

by

H. Morkoç

Materials Research Laboratory and
Coordinated Science Laboratory
104 South Goodwin Avenue
Urbana, IL 61801
e mail: morkoc@uiuc.edu

Abstract

Group III-V nitrides, notably GaN, have recently received a great deal of attention and accordingly a great deal of progress has been made. Violet, blue, green and yellow LEDs with outstanding performance are available. Electronics devices with very encouraging characteristics, with tremendous performance predictions, are beginning to appear in the literature. These highly productive device activities can not be supported without proper attention paid to deposition and characterization techniques. In this presentation, deposition of GaN and related heterostructures by MBE will be described backed by structural and other electronic characterization. The presentation will be complementary in nature to that by D. Reynolds.

In collaborations with Profs. Jiang and Lin at Kansas State, low temperature time-resolved photoluminescence emission spectroscopy has been employed to probe the free-excitonic transitions and their dynamic processes in GaN grown by molecular beam epitaxy (MBE). The exciton photoluminescence spectral lineshape, quantum yield, and recombination lifetimes have been measured at different excitation intensities and temperatures, from which the binding energies of the free and neutral-donor-bound excitons, the energy bandgap, and the free exciton radiative recombination lifetimes of GaN grown by MBE have been obtained. Our results have demonstrated the superior crystalline quality as well as ultra-high purity of the investigated sample, implying a new major breakthrough in MBE growth technologies for GaN.

Films with 45 arc seconds and 5 arc minutes rocking curves have been grown analyzed for their electrical, optical and structural properties, the latter with TEM and X ray diffraction. We find remarkable correspondence between the in-plane stacking order (coherence length and mosaic spread) and the electrical and optical properties. Contrary to common belief, our observations show unequivocally that the out-of-plane structural features, which are

considerably better developed than the in-plane counterparts, can not be used for determining the material quality with respect to optical and electrical activity. In particular, the (00L) mosaic spread is not a good indicator of film quality.

Quantization of band to band transition in a Si doped GaN/AlGaN quantum well was investigated. A good fit to the room temperature PL spectrum of the GaN quantum well studied was obtained using values 0.3 m_e and 0.19 m_e for the heavy hole and conduction electron effective masses, respectively, and a 67:33 conduction to valence band offset.

Photoluminescence spectrum of high quality GaN grown on SiC reveals that the optical transitions involving free excitons and donor bound excitons are red shifted compared to those observed in GaN grown on sapphire substrates. At T=4 K, photoluminescence peaks resulting from annihilation of donor bound excitons and free excitons were observed at 3.460 eV and 3.467 eV, respectively, as opposed to 3.477 and 3.483 eV observed in GaN on sapphire. This red shift can be accounted for with in plane residual tensile stress that in the GaN film, brought about by the difference in the coefficient of thermal expansion between the film and the substrate.

Optically pumped stimulated emission, in collaboration with Prof. J. J. Song whose group performed the optical pumping experiments, has been observed in separate confinement AlGaN/GaN heterostructures using a side pumping geometry. Evidence for stimulated emission was through spectral narrowing with increased pump power and superlinear increase of spontaneous emission intensity. It should be noted that the stimulated emission threshold depends on sample orientation. A threshold pump power of 80 kW/cm^2 was observed in a sample of the shape 100 μm wide strip and mediocre facets. The threshold value should be used as ballpark figure when comparing samples.

In this presentation, the details of the above activity will be described in some detail.

Abstract for Don Reynolds' 75th Birthday Symposium "Growth and Optical Properties of Compound Semiconductors". To be held in Dayton Ohio, November 13-14, 1995.

SiC and III-Nitrides Band Structure, Impurities and Superlattices

W.J.Choyke
Dept.of Physics and Astronomy
University of Pittsburgh
Pittsburgh,PA 15260, USA.

List of Collaborators: R.P.Devaty, L.L.Clemen, M.F.MacMillan, M.Yoganathan, G. Pensl, A.J.Steckl, W.R.L.Lambrecht, B.Segall, J.A.Edmond, J.A.Powell, D.J.Larkin, M.Asif Khan and J. Kuznia

Abstract

A systematic study of the vacuum uv-reflectivity (4-10 eV) for an electric field perpendicular to the c axis is presented for SiC polytypes. Experimental results for the 4H, 15R, 6H and 3C SiC polytypes are compared to the theoretical calculations within the local density approximation in conjuction with a muffin-tin-orbital basis set for the 2H, 4H, 6H and 3C polytypes. Agreement to ~ 0.2 eV is obtained between theoretical and experimental peak positions assuming a single, **k**-point, energy-, and polytype - independent gap correction. The main features and their trends with degree of hexagonality of the polytype are interpreted in terms of interband transitions involving extended regions in the Brillouin zone where the valance and conduction bands are nearly parallel.

More precise phonon energies at the positions of the conduction band minima in 4H SiC and 6H SiC have been obtained by means of high resolution 1.6K photoluminescence experiments. These experimental phonon energies have been compared with calculated

values at the **M**, **U**, and **L** points in the Brillouin zone. We conclude that the minima in 4H SiC are at the **M** point and that therefore 4H SiC has <u>three</u> conduction band minima. On the other-hand for 6H SiC it seem probable that the minima are at the **U** point and we therefore expect <u>six</u> minima for 6H SiC.

Erbium (Er^{3+}) 1.54μm luminescence has been measured in 4H, 6H, 15R and 3C SiC from 2K to 525K. The relative integrated luminescence intensity is given from 300K to 525K. Importantly, the relative integrated luminescence is substantially constant from 2K to 400K for the four polytypes measured. For 6H SiC, <u>five</u> additional higher energy spectra have been found which we attribute to higher lying Er^{3+} multiplets. We also report 1.54μm room temperature electroluminescence from erbium implanted 6H SiC. The electroluminescence spectrum is identical to the photo luminescence spectrum at room temperature. The integrated luminescence intensity measured from 1.49μm to 1.64μm begins to saturate above 0.5mA. The integrated electroluminescence intensity increases with the donor concentration of the samples up to the mid 10^{17} cm^{-3}.

AlN-GaN short period superlattice films have been studied by means of low temperature cathodoluminescence. Spectra are obtained at 6K, 77K and 300K. A broad ultraviolet peak is observed above the bandgap of GaN. Evidence is given that the shift of the peak of this ultraviolet luminescence arise from quantum confinement in the GaN layers of the superlattice. Furthermore, the room temperature infrared reflectance of the AlN-GaN short period super -lattice films has been measured in the region of the restrahl bands of AlN and GaN. The measured reflectance spectra are compared to calculated spectra using an effective medium theory to model the dielectric function of the superlattice. The optical properties of the individual materials making up the samples are modeled with Lorents oscillators using only bulk input parameters. Using this modeling technique, it is possible to obtain thickness estimates for the total superlattice film and the buffer layer.

Properties of III–V/II–VI Wide Band–Gap Semiconductor Materials

D.C. Reynolds *

University Research Center

Wright State University

Dayton, OH 45435

Interest in wide band–gap semiconductor materials has been increasing over the past few years. The main catalyst driving the renewed interest is the potential for high temperature electronics, as well as the potential for short wavelength display diodes and lasers. One promising wide band–gap material possessing the properties required for the above applications is GaN. The equilibrium crystal structure for GaN is the wurtzite structure. In high quality material, optical characterization will reveal much information pertinent to the energy band structure of the material. In GaN, one assumes that the bottom of the conduction band is predominantly formed from the s–levels of Ga and the upper valence band states are formed from the p–levels of N. The upper valence band states are constructed out of appropriate linear combinations of products of p_x,p_y,p_z–like orbitals with spin functions. In the absence of both spin–orbit and crystal field effects, these states are degenerate. The crystal field of the wurtzite lattice partially removes the degeneracy, separating the p_z orbital from the p_x and p_y orbitals. The p_x,p_y band is further split by spin–orbit coupling. If one assumes an approximately spherical potential in the neighborhood of the N atoms, the higher energy of the two spin states is the one in which the electron spin and the orbital angular momentum are parallel. This result is anticipated also from the atomic spin–orbit splitting, in which the $P_{3/2}$ state is known to

have a greater energy than the $p_{1/2}$ state.

The emission and reflection spectra of GaN have been investigated in the intrinsic region and the data have been interpreted in terms of the wurtzite crystal band structure. Three intrinsic exciton transitions have been observed, one associated with each of the valence bands. Exciton excited states associated with the two top valence bands were also observed. The exciton binding energies, the band–gap energies, the exciton Bohr radii are all reported along with the dielectric constant and the spin orbit and crystal field parameters for GaN.

One problem that has plagued the development of GaN is the lack of consistent high quality material. The techniques most recently used to grow GaN are molecular beam epitaxy (MBE) and metal organic chemical vapor deposition (MOCVD). The majority of material has been grown on sapphire substrates with some effort on Si, SiC, and GaAs. The lattice mismatch between the substrates and GaN is substantial; this leads to strain–induced defects and dislocations. ZnO is a material that is closely lattice matched to GaN and has the same crystal structure, as a result it offers potential as a substrate material on which high quality GaN may be grown. Very high quality ZnO has been grown, in platelet form, as will be demonstrated.

The results of optically pumped lasing from a ZnO platelet at low temperatures (2 K) and low pump power (~ 1 W/cm^2) is reported. The lasing cavity was an as–grown cavity where the bounding surfaces of the cavity are crystal planes. The sample was pumped with the 3250 Å line of a HeCd laser having an output power of 5 – 7 mW. Normalizing the output power to a beam diameter of 1.2 mm gives a pump power of ~1 W/cm^2. Extremely well formed lasing modes were observed from which a changeover from absorption to emission could be clearly detected. The lasing structure reflects very high quality crystal structure as well as very well formed cavity structure.

* Work was performed at Wright Laboratory, WL/EL, Wright Patterson Air Force Base under USAF Contract No. F33615-95-C-1619

SPVT™ The Economical II-VI Growth Method

by

Bill Harsch & Gene Cantwell

Eagle-Picher Ind., Inc.

II-VI compound semiconductor devices have been researched, developed, prototyped, and, under some extreme conditions, manufactured for a variety of applications. Except for a few notable projects, these devices have never been commercially produced in any large quantities or reasonable prices. Because of this, II-VI materials have been given the reputation of being the expensive alternative to other optoelectronic materials.

Eagle-Picher produced II-VI crystals, substrates and various devices manufactured from II-VI single crystals for over forty (40) years. It was during this time that EP determined that the high cost of II-VI materials was primarily in the yield of usable material during crystal growth and subsequent processing. For the last ten (10) years, EP has been working to improve the yields of the preferred process of physical vapor transport growth (a method pioneered by Don Reynolds). The culmination of this work has produced a process called Seeded Physical Vapor Transport (SPVT™), a growth process that yields almost 100% usable material in 2" and 3" diameters. A unique aspect of the SPVT™ process is that the crystals can be grown at full diameter over the entire length of the ingot. Nearly the entire length of the crystal is usable at the full diameter since the crystalline quality improves to that of the bulk crystal within 1-3 mm of the seed. Not only have the yields improved, but the quality is unsurpassed, producing material with as few as 650 dislocations/cm^2, X-ray FWHM of <15 arc seconds, no twins, no slip and no low angle grain boundaries.

SPVT crystals have been grown of ZnSe, CdTe, ZnTe, CdS, ZnSeS, ZnCdSe, CdSSe, CdSeS, CdZnTe, CdTeSe, and ZnO. High quality ZnSe substrates combined with MBE of ZnSe have produced homoepitaxial wafers that are used to produce low cost LED's in wavelengths of 485 nm and 512 nm. The same homoepitaxial approach is being used to develop a 505 nm laser diode (LD). Cost analysis of the manufacturing process for the production of LED's show that the material costs are between $0.006 and $0.018.

Excitonic Molecules in II-VI Compounds
-- Past, Present and Future

Shigeo Shionoya*

The formation of excitonic molecules (biexcitons) in II-VI compounds was first observed in CdS by the author's group[1] in 1972 by measuring luminescence spectra under high intensity excitation. The optical conversion from single excitons to excitonic molecules was also observed, and the giant oscillator strength effect was confirmed. Since then, excitonic molecules were observed in ZnO, ZnSe, ZnTe and CdSe.

Recently excitonic molecules in ZnSe-based quantum wells were observed by two research groups.[2,3] It was found that the binding energy of molecules is remarkably enhanced in two dimensional well structures. This fact was in agreement almost quantitatively with results of theoretical calculations for the binding energy of excitonic molecules in low dimensional systems. This seems to indicate that the formation of excitonic molecules in such systems is possible at room temperature.

The system of excitonic molecules is an ideal 4-level laser system. Then the author suggests to attempt to fabricate ZnSe-based blue semiconductor lasers with high performance by utilizing excitonic molecules in low dimensional structures. The most crucial point to be discussed is whether population inversion between single excitons and excitonic molecules is realized even at room temperature. Very recently Sugawara[4] performed a

theoretical analysis of this point. His conclusions are that in the case of free excitonic molecules population inversion is possible only at low temperatures, but that in the case of localized excitonic molecules at certain potentil minima in well planes it is possible to achieve population inversion even at room temperature provided local potentials are deep enough. By theoretical calculations he showed that the excitonic molecule transition is expected to produce enough optical gain for lasing, and that the fabrication of semiconductor lasers with low threshold current is possible. Further in these kinds of lasers one may expect high differential quantum efficiency close to one, because the concentration of free carriers which prevents the quantum efficiency to be high should be very low.

The author really hopes that blue semiconductor lasers utilizing localized excitonic molecules with extremely high performance are realized in the near future.

1)S. Shionoya, H. Saito, E. Hanamura and O. Akimoto, Solid State Commun. 12 (1973) 223.

2)Q. Fu, D. Lee, A. Mysyrowicz, A. V. Nurmikko, R. L. Gunshor and L. A. Kolodziejski, Phys. Rev. B 37 (1988) 8791.

3)Y. Yamada, T. Mishina, Y. Masumoto, Y. Kawakami, S. Yamaguchi, K. Ichino, Sz. Fujita, Sg. Fujita and T. Taguchi, Phys. Rev. B 52 (1995) 2596.

4)M. Sugawara, Jap. J. Appl. Phys. to be published.

x Foremerly at The Institute for Solid State Physics, The University of Tokyo.

Abstracts

(Contributed Papers)

Surfactant-Mediated Growth of AlGaAs By Molecular Beam Epitaxy

R. Kaspi, D.C. Reynolds
University Research Center, Wright State University, Dayton, OH 45435

J. Brown, K.R. Evans
Wright Laboratory, Solid State Electronics Directorate (WL/ELR),
Wright-Patterson AFB, OH 45433;

We have explored the use of Sb as an isoelectronic surfactant during the growth of $Al_xGa_{1-x}As$ layers by solid source MBE. A steady-state population of surface-segregated Sb was maintained at the film surface by providing a continuous incident Sb_2 flux during deposition. For a given set of growth conditions, the amount of Sb at the surface was measured in-situ by line-of-sight mass spectrometry and was shown to be most easily controlled by varying the incident Sb_2 flux.

When Sb is used a surfactant, photoluminescence (PL) analysis of the bandedge indicated a significant improvement in the optical quality of $Al_{0.22}Ga_{0.78}As$ layers deposited at 690°C. For the optimal case, a ~20-fold increase in the bound exciton peak intensity was accompanied by a reduction in the FWHM from 8.0 to 2.6 meV. In addition, surfactant-mediated growth of AlGaAs resulted in reduced surface roughness, and smoother inverted interfaces with GaAs as evidenced by sharper and more intense GaAs PL peaks from AlGaAs/GaAs(250Å)/AlGaAs quantum well structures. Evidence for enhanced surface diffusion kinetics in the presence of Sb was given by prolonged reflection high-energy electron diffraction intensity oscillations.

ELECTRONIC AND GROUND STATE PROPERTIES OF BINARY SEMICONDUCTOR COMPOUNDS

P.E. Van Camp and V.E. Van Doren

Department of Physics, University of Antwerp (RUCA)

Groenenborgerlaan 171, B-2020 Antwerpen, Belgium

Ab-initio calculations in the framework of Density Functional and Pseudopotential Theory are carried out of the electronic structure, the charge density and the total energy of binary semiconductor compounds under hydrostatic and uniaxial pressure. These compounds are small gap (such as GaAs) as well as wide gap (such as GaN) semiconductors. The calculations are done mostly in the local density approximation, i.e. Kohn-Sham exchange and Ceperley-Alder correlation. However, also non-local density functionals consisting of an exponentially and a Gaussian screened Coulomb interaction have been used to calculate the band gap in the main symmetry points. For several cases, the transition pressure from one structure to another is determined as well as the pressure coefficients of the main band gaps. It is shown that several properties are calculated with adequate accuracy to be compared with experiment, so that values which have not yet been measured are trustworthy predictions.

Gallium Selenide Crystals for Far-IR NLO Applications

by

N. Fernelius and F. K. Hopkins
Materials Directorate, Wright Laboratory, AFB, OH 45433

and

N.B. Singh, T. Henningsen, V. Balakrishna, and R. Narayanan*
Westinghouse Science and Technology Center, Pittsburgh, PA 15235

ABSTRACT:

Gallium Selenide has very favorable nonlinear optical properties, wide transparency range, reasonably high thermal conductivity compared to other NLO crystals and high melting temperature. Application of GaSe in optical devices is limited due to unavailability of fabricable crystals. We have developed a method to synthesize large-batch sizes of GaSe and have grown single crystals by the Bridgman method. Our results showed a d value of 75 pV/m for GaSe. GaSe crystals were tested by using 9.6 micrometer wavelength, at a fluence of 1.6 J/cm^2 and 140 MW/cm^2 without damage. The 2-mm thick crystal was used in a high-power test where a crystal with an AR coating was able to operate at 30 KHz with an average power of 21 W into the crystal, equivalent to 32 KW/cm^2 CW in a 100 micrometer spot.

*Department of Chemical Engineering, University of Florida, Gainsville, FL

Infrared Transmission Topography: Application to Nondestructive Measurement of Dislocation Density and Carrier Concentration in Silicon-Doped Gallium Arsenide Wafers

M.G. Mier[1], D.C. Look[2], J.R. Sizelove[1], D.C. Walters[2], and D.L. Beasley[1]
1. Solid-State Electronics Directorate, Wright Laboratories, WL/ELDM, Wright-Patterson Air Force Base, OH, 45433-7323
2. University Research Center, Wright State University, Dayton, OH 45435

Devices made on bulk GaAs:Si wafers may be critically dependent on both low dislocation density and high free carrier concentration in the material. Standard techniques for measuring these quantities are destructive: e.g., carrier concentration measurement by Hall effect generally requires small pieces and ohmic contacts, while dislocation counting requires etching the wafer to delineate etch pits where dislocations intersect the surface, and this process destroys the wafer surface finish. We report here a nondestructive method for measuring these quantities. For GaAs:Si with $n_{avg} = 1.7 \times 10^{18} cm^3$, we find that at a wavelength of 0.9 μm we get ~2% transmission, sufficient for a high-contrast topographic map of dislocation density as well as background carrier concentration. A similar measurement at a slightly longer wavelength 1.0 - 1.5μm gives 20 - 40% transmission and provides even better data for a topographic map of free carrier concentration. The latter data have been calibrated by Hall effect measurements and the former by etching the wafer in molten potassium hydroxide (450°C for ~45 minutes) and counting the resulting etch pits. We attribute the unprocessed wafer transmission variations to free carrier variations for $\lambda > 1.0\mu m$ and free-carrier-induced bandgap variations for $\lambda < 1.0\mu m$. Our correlation plot at $\lambda > 1.5\mu m$ gives $n = 1.91 \times 10^{17} \alpha + 2.35 \times 10^{17}$, where α is the optical absorption in cm^{-1} and n is the free carrier concentration in cm^{-3}. At the wavelength $\lambda = 0.9\mu m$, we correlate the optical absorption with the counted etch pit density, giving $\rho_o = -4.60 \times 10^2 \alpha + 2.24 \times 10^4$, where α is again the optical absorption and ρ_o is the etch pit density in cm^{-2}.

Photoresponse Studies of the Polarization Dependence of the $CdGeAs_2$ Band Edge, Gail J. Brown and Melvin C. Ohmer,Wright Laboratory, Materials Directorate, Wright Patterson AFB, OH, and Peter G. Schunemann, Lockheed Sanders, Nashua, NH

Fourier Transform mid-infrared photoresponse studies were performed on an oriented p-type cadmium germanium arsenide uniaxial crystal. The effects of optical polarization alignment, parallel and perpendicular to the c-axis of the crystal, were studied, as well as the effects of the transport electric-field direction. The measured optical band edge was 0.578 eV at 9K for all polarization and bias configurations. This band gap energy is in good agreement with absorption and photoluminescence results for this sample. However, at 240K, the photoresponse onset varied from 0.53 eV to 0.50 eV as the optical polarization was switched from perpendicular to parallel to the c-axis. This difference in the near room temperature activation energy of the photoresponse is attributed to deep native defect levels near the band edge. These deep defect levels have a stronger photoresponse when the optical polarization is parallel to the c-axis. These deep levels at times obscure the true band edge and can cause under estimates of the band gap energy. By studying the photoresponse spectra as a function of polarization and temperature, the separation of deep level and band gap transitions can be made. These results can help to explain the wide disparity in the reported $CdGeAs_2$ band gap in the Russian literature. In addition, the intensity of the photoresponse was found to be only slightly dependent on the optical polarization direction, but strongly dependent on the bias electric-field direction. The largest photoreponse was observed when the optical polarization was parallel to the c-axis and the bias electric field was perpendicular to the c-axis. The bias electric-field direction also had a significant effect upon the temperature dependence of the peak photoresponse intensity. $CdGeAs_2$ has possibly the largest second order non-linear susceptibility of any birefringent compound semiconductor appropriate for efficient second harmonic generation of CO_2 laser wavelengths. At present, its performance at room temperature is limited by extrinsic absorption due to native defects.

Monitoring and Control During MBE by Desorption Mass Spectrometry

K. R. Evans, R. Kaspi, C. R. Jones, and J. E. Ehret
Solid State Electronics Directorate, Wright Laboratory
Wright-Patterson Air Force Base, Ohio 45433-7323

Desorption mass spectrometry (DMS) is an in-situ sensor technique which provides a quantitative measure of desorption events during MBE growth processing. DMS is non-destructive, has a rapid associated response-time, is simple to calibrate and keep calibrated, requires very simple signal processing, and provides a wealth of information about growth chemistry. We review the application of DMS for real-time sensing of growth rate, alloy composition, shutter events, flux drift, surface reconstruction, surface-riding population, and heterointerface abruptness; and the recent incorporation of DMS in real-time feedback loops for the controlled production of arbitrary vertical composition profiles.

Self-consistent k.p band structure calculation for AlGaAs/InGaAs pseudomorphic high electron mobility transistors

B. Jogai
University Research Center
Wright State University
Dayton, OH 45435

Abstract

A self-consistent four-band k.p calculation for the band structure of AlGaAs/InGaAs pseudomorphic high electron mobility transistors (p-HEMTs) is presented. The eigenstates are described in a basis consisting of electron, heavy-hole, light-hole, and split-off states of the host bulk material. The k.p Hamiltonian derived in this basis includes strain-induced mixing between the conduction and light-hole and conduction and split-off bands. It also includes additional splitting between the heavy- and light-hole bands, apart from that induced by the shear deformation potential, caused by strain-induced changes in the spin-orbit interaction. The Hartree potential is calculated from the Poisson equation and the exchange-correlation potential from density-functional theory within the local density approximation. The model calculation accounts for deep level surface acceptor and donor states, both of which contribute to Fermi-level pinning at the surface. Also included are acceptor interface states at the inverted GaAs/AlGaAs interface. The present calculation has been used as a characterization tool to analyze optical and Hall data from preprocessed p-HEMT material, since conduction-valence subband separations and mobile sheet charge densities are results of the calculation. The calculated energy differences and oscillator strengths between first and second electron subbands and the first heavy-hole subband transitions correlate very well with photoluminescence (PL) data.